# A Robust ToA and Pulse Width Estimator for Electronic Warfare Applications

Aline Silva, Bruna Luisa, Rafael Serra, Luiz Eugênio Segadilha, Sergio Neves and Jean Marc-Lopez

***Abstract*— We propose a robust Time of Arrival (ToA) and Pulse Width (PW) estimator for Electronic Intelligence and Electronic Support Measures systems in Electronic Warfare applications. Robust ToA and PW measurements of the intercepted radar pulse are assets in EW algorithms and are worthy to be pursued. The proposed estimation method is based on Autoconvolution and Model Change Detection theory. Computer simulations show the superior performance of the proposed method in the presence of AWGN and spurious signals when compared to two different Threshold methods and to an Autoconvolutional method. A comparison of the methods with a recorded radar pulse confirms the robustness of the proposed method in a real scenario.**

***Keywords*— Radar pulse width estimation, pulse parameters estimation, Time of arrival estimation, model change detection, autoconvolution, ELINT, Electronic Warfare, Electronic Support Measures (ESM).**

## I. Introduction

Blindly estimating intercepted radar pulse's parameters is one of the most important tasks of Electronic Warfare (EW) systems [1], particularly for Electronic Intelligence (ELINT) [2] and Electronic Support Measures (ESM) systems. It allows correct identification of the received radar waveform, that in turn, yields crucial information for predicting the mode of the enemy's operation and correctly performing pulse deinterleaving and threat sorting [3], [4].

However, this can only be properly executed if the pulses' Time of Arrival (ToA) and Pulse Width (PW) are well estimated. From the EW prospect, the best ToA and PW estimation method provides the correct time frame in which frequency measurements can be accurately made, regardless SNR at reception or pulse distortion, caused by emitter's degradation, multipath or spurious signals as interference, or jammers for example. The probability of detecting intrapulse modulation correctly dependes on the analysed time-frame [5]. A system model for intrapulse analysis is depicted in Fig. 1.

Historically, in analog EW equipments, a threshold is used to determine the pulse width. Until the present days, heuristics based on thresholds are used, even in the context of digital data [6]–[8]. But threshold methods are very susceptible to noise, multipath and emitter's degradation, motivating the research of robust PW estimation methods which convey the EW needs [9]–[11].

Aline Silva, Bruna Luisa, Rafael Serra, Luiz Eugênio Segadilha, Sergio Neves, Instituto de Pesquisas da Marinha (IPqM), Rio de Janeiro, Brazil, e-mails: {aline.oliveira, bruna.luisa, rafael.serra, luis.eugenio, sergio.neves}@marinha.mil.br; Jean-Marc Lopez, DGA-Technique Navale, Toulon, France, e-mail: jean-marc1.lopez@intradef.gouv.fr

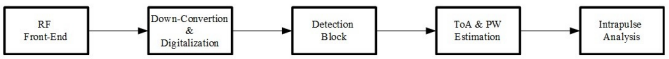


Fig. 1. System model for intrapulse analysis.

In this paper, we propose a robust method for ToA and PW estimation based on a combination of Model Change Detection theory and Autoconvolution, named here the AC-MCD method. The proposed method uses the autoconvolution of the received signal to approximately determine the middle point of the pulse in order to divide the processing interval into two segments. Then we apply MCD theory to determine the instant at which a DC level change occurs in each segment. The first jump instant is the estimated ToA and the interval from the first jump to the second jump is the estimated PW.

We compare the proposed method with two threshold-based methods [6], [11] and a convolution-based method [9], [10]. Computer simulations show the superior performance of the proposed method in the presence of AWG noise and distortion caused by a spurious signal. This latter feature is illustrated with a real pulse case. The term robust is loosely employed throughout this paper meaning the methods capacity of maintaining their PW estimates of corrupted or distorted pulses similar to the non-corrupted case.

This paper is organized as follow: the system model is explained in Section II, the proposed method is described in Section III; an overview of the other PW estimation methods is reviewed in Section IV, computer simulations are presented in Section V and, finally, conclusions are given in Section VI.

## II. System Model

Assume that the signals received from a wideband receiver of bandwidth $W$ after downconversion go through a high speed analog to digital converter (ADC), with sampling frequency, $f_s$, larger than $2W$ in order to avoid aliasing. The digital sequence is divided into Data Processing Interval (DPI) frames of $L$ samples each. Length $L$ is chosen accordingly, depending on the minimum and maximum expected radar pulse width and maximum Pulse Repetition Frequency (PRF), in order to accommodate only one radar pulse per DPI.

The DPI signal, $r(i)$, is described as

$$r(i) = r(t)|_{t=(i-1)t_s},\ i = 1, \ldots, L, \tag{1}$$

where $t_s = 1/f_s$ and $r(t)$ given hypothesis $\mathcal{H}_1$ (presence of radar pulse), is

$$r(t) = s(t - T) + n(t), \tag{2}$$

where $n(t)$ is the receiver thermal noise random process with autocorrelation function $R(\tau) = \sigma_n^2 \delta(\tau)$ and $s(t)$ is the radar pulse, which starts at instant $t = T$, given by

$$s(t) = Ag(t)\cos(2\pi f_c t + \rho(t) + \psi), \tag{3}$$

where $A$ is a constant that accounts for the signal amplitude, $f_c$ is the downconverted radar carrier frequency, $g(t)$ is the low-pass transmitted pulse envelope of duration $\tau$, $\rho(t)$ represents the phase or frequency modulation and $\psi$ is the initial phase.

The analytical signal, $r_a(i)$, is given by

$$r_a(i) = r(i) + j\mathcal{H}\{r(i)\}, \; i = 1, \ldots, L \tag{4}$$

where $\mathcal{H}\{x\}$ denotes the Hilbert transform of $x$. The magnitude $z(i)$, of $r_a(i)$, which is the envelope of the DPI, is given by

$$z(i) = |r_a(i)|. \tag{5}$$

The definition of intrapulse signal-to-noise ratio (SNR) adopted in this paper is

$$\text{SNR} = 10\log_{10}\left(\frac{A^2}{2\sigma_n^2}\right). \tag{6}$$

The DPIs go through a detection block which indicates the presence or absence of a radar pulse within it. DPIs with affirmative indication of pulse go through the pulse parameters estimation block, in which is located the proposed ToA and PW estimation method. These parameters are used to select the frame which enters the intrapulse analysis block, where the modulation and other parameters are estimated. This process is depicted in Fig. 1.

## III. Proposed AC-MCD ToA and Pulse Width Estimation Method

The PW estimation problem can be modelled as the problem of determining two unknown jump instants of DC levels, which are also unknown. Fig. 2 illustrates this idea. Detecting the change time of a DC level is a well established branch in Model Change Detection (MCD) theory.

The drawback of the MCD applied to three DC levels is its high computational complexity, in the order of $\mathcal{O}(L^3)$, where $L$ is the length of the data processing interval (DPI) [12]. A way of reducing its computational complexity is by implementing it with dynamic programming, which involves some contour conditions and may get tricky. The computational complexity of the proposed method is $\mathcal{O}(L^2)$ and its implementation is very simple.

The proposed method combines an autoconvolution of the DPI MCD theory. The $k$-th element of $y(i)$, which is the result of the autoconvolution of the signal envelope within the DPI, $z(i)$, $i = 1, \ldots, L$, is given by

$$\begin{aligned} y(k) &= \sum_{j=1}^{L} z(j)z(k-j+1), \\ k &= 1, \ldots, 2L-1, \\ j &= 1, \ldots, k. \end{aligned} \tag{7}$$

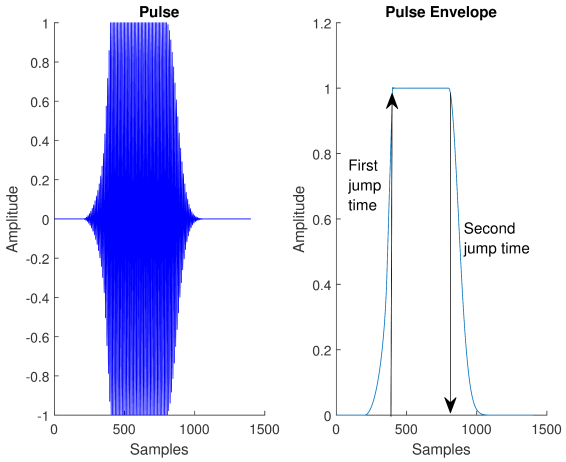


Fig. 2. Example of applying MCD for PW estimation.

The time index, $i^*$, at which we divide $z(i)$ into two segments is

$$i^* = \left\lfloor \frac{k^*}{2} \right\rfloor, \tag{8}$$

where $k^*$ is the time index for which $y(k)$ is maximum. For monotonic rising and falling pulse edge functions and no noise, $i^*$ in (8) is exactly the middle point of the pulse [10]. In the presence of noise, for positive signal to noise ratio (SNR), $i^*$ is a good approximation of the middle point.

Once we have obtained $i^*$, we divide $z(i)$ into two segments, $z_L(i)$ and $z_R(i)$, given by

$$z_L(i) = z(i), \; i = 1, \ldots, i^* \tag{9}$$

$$z_R(i) = z(i^* + i), \; i = 1, \ldots, L - i^*. \tag{10}$$

This process is depicted in Figs. 3, 4 and 5. Fig. 3 depicts a decentralized pulse envelope. Fig. 4 depicts the autococonvolution of the pulse envelope depicted in 3 and its point of maximum. Fig. 5 depicts the pulse envelope again and the position of the point given by (8). One can see from Fig. 5, that the autoconvolution procedure works for finding the middle point even when the pulse is decentralized. The curve from the beginning of the pulse until point $P$ in Fig. 5 is $z_L(i)$ and from $P+1$ to the end is $z_R(i)$.

In a second step, we want to detect the jump time of the DC level for the two segments, $z_L(i)$ and $z_R(i)$. If $A_0$ and $A_1$ were known we would select $n_0$ as the instant $n$ which minimizes the average deviation of the data from: $A_0$, over the interval before the jump, and $A_1$, over the interval after the jump. Since they are not known, we substitute them by their estimate and, therefore, minimize the cost function, $J(n_0)$,

$$J(n_0) = \sum_{n=1}^{n_0-1} \left(z(n) - \hat{A}_0\right)^2 + \sum_{n=n_0}^{L} \left(z(n) - \hat{A}_1\right)^2, \tag{11}$$

where

$$\hat{A}_0 = \frac{1}{n_0 - 1} \sum_{i=1}^{n_0-1} z(i), \tag{12}$$

$$\hat{A}_1 = \frac{1}{L - n_0 + 1} \sum_{in_0}^{L} z(i). \tag{13}$$

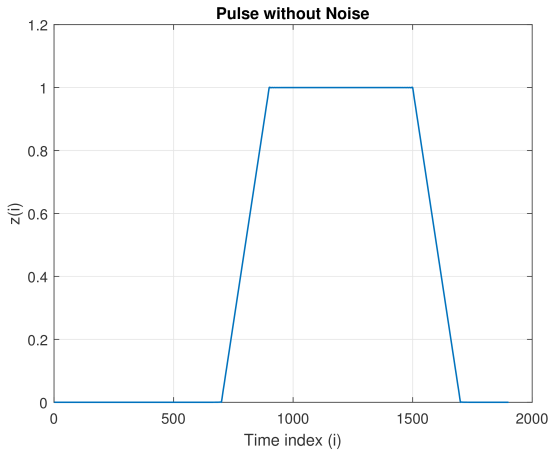


Fig. 3. Pulse envelope without noise.

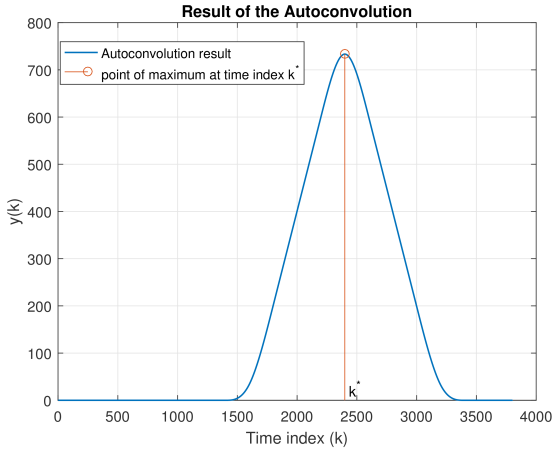


Fig. 4. Result of the autoconvolution of the pulse envelope.

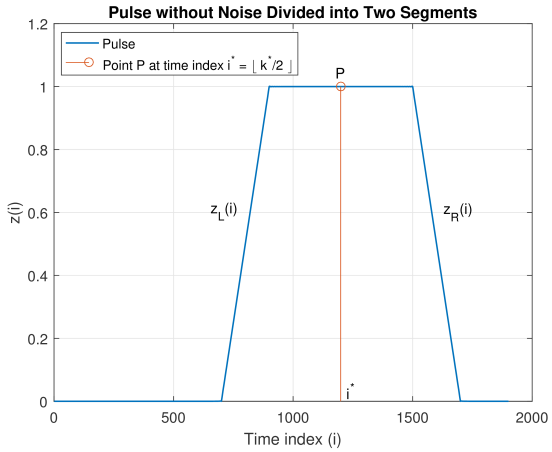


Fig. 5. Pulse envelope divided into two segments.

The estimated PW, $\hat{\text{PW}}$, in sample units, is, thus, computed as

$$\hat{\text{PW}} = i^* - n_L + n_R, \tag{14}$$

where $i^*$ is defined in (8) and $n_L$ and $n_R$ are the output of the minimization problem in (11) applied to the left and right parts of the pulse respectively, $z_L(n)$ and $z_R(n)$. Note that $n_L$

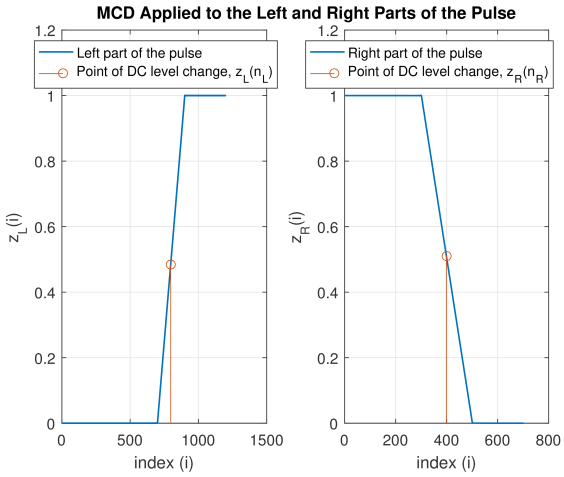


Fig. 6. MCD applied to the left and right parts of the pulse.

is the ToA sample estimate

$$\hat{\text{ToA}} = n_L. \tag{15}$$

The jump times $n_L$ and $n_R$, which are the results of the minimization problem (11) applied to the left and right parts of the pulse $z_L(n)$ and $z_R(n)$ are depicted in Figs. 5 and 6 respectively.

## IV. Overview of other Pulse Width Estimation Methods

This section presents an overview of the methods adopted in this paper for comparison: the Histogram-Based Threshold method [6], the Mean-Based Threshold method [11] and the Autoconvolutional method [10].

### A. The Histogram-Based Threshold Method

In this method, two amplitude levels of the received pulse envelope, $z(i)$, $i = 1, \ldots, L$, are computed by means of constructing the histogram of $z(i)$ [6]. The histogram peak to the left is the noise level estimative and the peak to the right is the signal level estimative. A threshold is computed as the median of these two levels. The pulse width is then computed as the total number of samples within the DPI which exceed the threshold. Note that this method does not provide the ToA.

### B. The Mean-Based Threshold Method

In this method proposed in [11], a threshold is computed as the median value of the maximum and minimum value of $z(i)$, $i = 1, \ldots, L$. Then, the amplitude level is computed as the arithmetic mean of all samples within the DPI which exceed the threshold and the noise level is computed as the arithmetic mean of all samples within the DPI which do not exceed the threshold. Then a new threshold is computed as the median value of the amplitude and noise levels. The pulse width is then measured as the total number of samples which exceed this new threshold and also satisfy the continuity criterion, which is defined in [11] as the samples above the threshold whose neighbors also exceed the threshold. Note that this method does not provide the ToA.

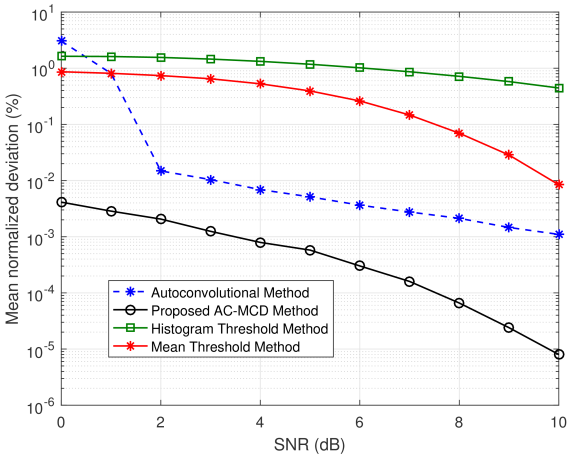


Fig. 7. Mean Normalized Deviation.

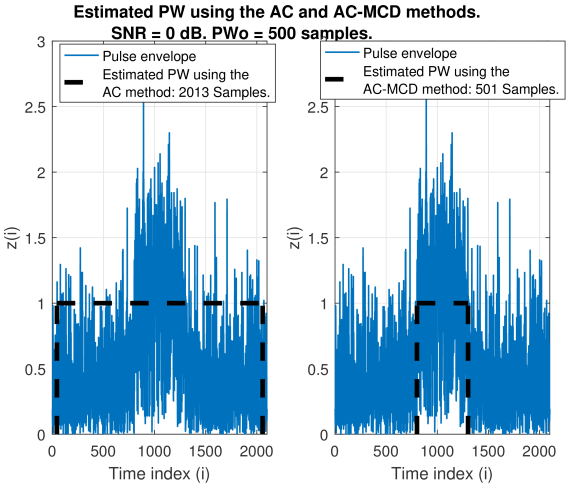


Fig. 8. Example of the estimated ToA and PW of the AC (left) and proposed AC-MCD (right) methods for SNR = 0 dB.

### C. The Autoconvolutional Method

The Autoconvolutional method presented in [10] is summarized here. First, one determines $i^*$ as described in (8) and generates the left and right segments $z_L(i)$ as in (9) and $z_R(i)$ as in (10). Then, one performs the autoconvolution of $z_L(i)$ and $z_R(i)$, producing $y_L(i)$ and $y_R(i)$ respectively. The estimated PW using the autoconvolutional method, $\hat{\text{PW}}_{\text{AC}}$, may be written as

$$\hat{\text{PW}}_{\text{AC}} = 2i^* - n_L^* + n_R^*, \tag{16}$$

where $n_L^*$ is the index for which $y_L(n)$ is maximum and $n_R^*$ is the index for which $y_R(n)$ is maximum. Note that $n_L^*$ is the ToA sample.

## V. Simulation

In this section we compare the presented methods in terms of robustness in the presence of AWG noise. The simulated pulse has a rectangular envelope with a pulse width of 500 samples ($\text{PW}_0 = 500$). The pulse is located in the center of a Data Processing Frame (DPI) of 2100 samples. The metric used for assessing the robustness is the mean normalized deviation, $\epsilon$, defined as

$$\epsilon = \frac{1}{N}\sum_{i=1}^{N}\frac{|\hat{\text{PW}} - \text{PW}_0|}{|\text{PW}_0|}, \tag{17}$$

where $\hat{\text{PW}}$ is the estimate and $\text{PW}_0$ is the correct reference value. The comparison with 500 Monte Carlo trials ($N = 500$) for each SNR value (Eq. (6)) is depicted in logscale in Fig. 7. From Fig. 7 one can see the superior robust performance of the proposed method. The Autoconvolution (AC) method [9], [10], except for very low SNRs, is better than the Threshold Histogram-Based [6] and Mean-Based [11] methods . Fig.8 depicts the estimated combination of ToA and pulse width of one Monte Carlo trial using the AC and the proposed AC-MCD methods for 0 dB SNR. From Fig. 8 it is clear that only the proposed method is able to produce reliable results for all SNR range.

Figs. from 9 to 14 illustrate another important desired feature of PW estimation methods for EW applications: the capacity of rejecting distortions caused by multipath or spurious signals. We simulated a pulse envelope based on the ADSR (Attack-Decay-Sustain-Release) model [13], [14] and added a shorter spurious pulse at its end and compared the output of the presented methods, without noise, for different heights of the spurious signal. When the amplitude of the spurious signal is not very high, all four methods are able to reject the spurious signal and behave as depicted in Fig. 9. When the amplitude of the spurious signal is very high, all four methods incorporate the spurious width to the correct pulse width, as depicted in Fig. 10. The results for the proposed AC-MCD, AC, Histogram and Mean-based threshold methods for an intermediate amplitude are depicted in Figs. 11, 12, 13 and 14 respectively. Though the threshold based methods do not estimate the ToA, for illustration purpose we have depicted their results in Figs. 13 and 14 using the ToA resulted from the proposed AC-MCD, which happens to be equal to the AC method for these examples. From Figs. 11 to 14 one can see that the proposed AC-MCD method has a superior capacity of rejecting the spurious signal.

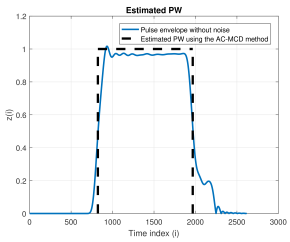


Fig. 9. Common behavior for low height spurious signal.

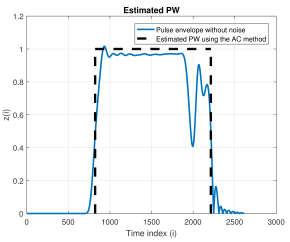


Fig. 10. Common behavior for high height spurious signal.

Figs. 15 and 16 depict the application of the AC and the proposed AC-MCD method to a real pulse with a non-theoretical amplitude profile. We have recorded this pulse from a sailing ship using an TEKTRONIX oscilloscope in association with a cornet antenna near a bay. From Figs. 15

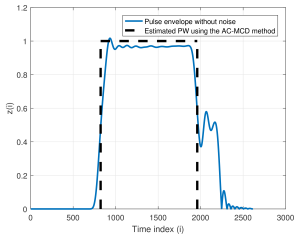


Fig. 11. AC-MCD method.

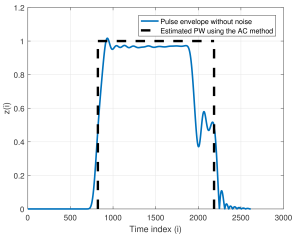


Fig. 12. AC method.

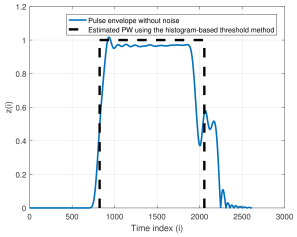


Fig. 13. Histogram-Based Threshold method.

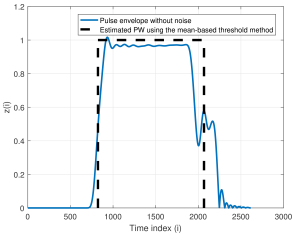


Fig. 14. Mean-Based Threshold method.

and 16 one can see that the proposed AC-MCD method rejects the spurious part of the recorded pulse while the AC method does not.

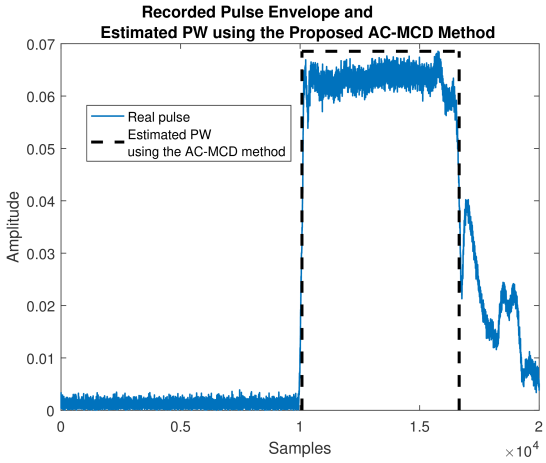


Fig. 15. Estimated PW using the proposed method in a real pulse.

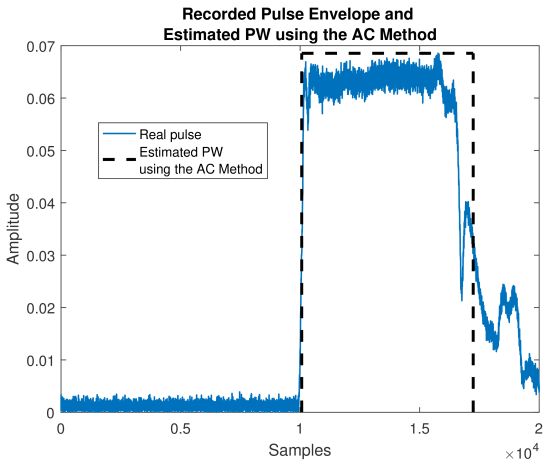


Fig. 16. Estimated PW using the AC method in a real pulse.

## VI. Conclusion

In this paper, we have proposed a robust ToA and pulse width estimator based on Autoconvolution and Model Change Detection theory, the AC-MCD method. We have compared its pulse width estimation performance with three other pulse width estimators in the presence of AWGN, namely, the threshold histogram-based [6], the threshold mean-based [11] and the autoconvolutional (AC) [10]. The proposed method shows superior performance and robustness with remarkable results for very low SNRs. The proposed method also filters out distortions caused by spurious signals, manifesting to be robust to non-theoretical pulse shapes. This is a very interesting feature to applications in EW and ELINT.

## Referências

[1] D. Curtis Scheleher, *Introduction to Electronic Warfare*, Artech House, 1986.

[2] Richard G. Wiley, *Electronic Intelligence: The Analysis of Radar Signals*, Artech House, second edition, 1993.

[3] J. Matuszewski, "The analysis of modern radar signals parameters in electronic intelligence system," in *2016 13th International Conference on Modern Problems of Radio Engineering, Telecommunications and Computer Science (TCSET)*, 2016, pp. 298–302.

[4] James Tsui and Chi-Hao Cheng, *Digital Techniques for Wideband Receivers*, Scitech Publishing an imprint of the IET, 3 edition, 2016.

[5] M. Jawad, Y. Iqbal, N. Sarwar, and F. A. Siddiqui, "Modulation characteristics analysis of the LPI radar pulses under non-cooperative estimation," in *2019 16th International Bhurban Conference on Applied Sciences and Technology (IBCAST)*, 2019, pp. 943–946.

[6] Pulses IEEE Standard for Transitions and Related Waveforms, *IEEE Std 181-2011 (Revision of IEEE Std 181-2003)*, Sep. 2011.

[7] TEKTRONIX, *Fundamentals of Radar Measurements*, https://download.tek.com/document/37W_22065_4_Radar_PR.pdf.

[8] ROHDE SCHWARZ, *RF Pulse Measurements in time and frequency domains with VSE-K6*, https://scdn.rohde-schwarz.com/ur/pws/dl_downloads/dl_application/application_notes/1ma249/1MA249_1e_PulseMeasTFDomain.pdf.

[9] B. H. Lee, R. Inkol, and F. Chan, "Estimation of pulse parameters by convolution," in *2006 Canadian Conference on Electrical and Computer Engineering*, 2006, pp. 17–20.

[10] Y. T. Chan, B. H. Lee, R. Inkol, and F. Chan, "Estimation of pulse parameters by autoconvolution and least squares," *IEEE Transactions on Aerospace and Electronic Systems*, vol. 46, pp. 363–374, 2010.

[11] M. A. Zanina, A. A. Belov, and S. V. Volvenko, "Estimation of accuracy of algorithm for measuring radiofrequency pulse parameters," in *2018 IEEE International Conference on Electrical Engineering and Photonics (EExPolytech)*, 2018, pp. 98–102.

[12] Steven M. Kay, *Fundamentals of Statistical Signal Processing: Detection theory*, vol. II of *Prentice-Hall Signal Processing Series*, Prentice-Hall, 1998.

[13] H. G. Kim, N. Moreau, and T. Sikora, *Introduction to MPEG 7 Audio*, Hoboken, NJ, USA: John Wiley and Sons, 2005.

[14] R. S. Figueirêdo, F. A. Carijó, and J. C. Pires-Filho, "Geração de cenários radar arbitrários baseada em palavras descritoras de pulsos," in *XIX SIGE - Simpósio de Aplicações Operacionais em Áreas de Defesa - São José dos Campos/SP - Brasil*, 2017.